International Journal of Mechanical, Industrial and Aerospace Sciences
ISSN: 2517-9950
Vol:9, No:11, 2015

Dynamic Simulation of IC Engine Bearings for Fault Detection and Wear Prediction

M. D. Haneef, R. B. Randall, Z. Peng

***Abstract*—**Journal bearings used in IC engines are prone to premature failures and are likely to fail earlier than the rated life due to highly impulsive and unstable operating conditions and frequent starts/stops. Vibration signature extraction and wear debris analysis techniques are prevalent in industry for condition monitoring of rotary machinery. However, both techniques involve a great deal of technical expertise, time, and cost. Limited literature is available on the application of these techniques for fault detection in reciprocating machinery, due to the complex nature of impact forces that confounds the extraction of fault signals for vibration-based analysis and wear prediction.

In present study, a simulation model was developed to investigate the bearing wear behaviour, resulting because of different operating conditions, to complement the vibration analysis. In current simulation, the dynamics of the engine was established first, based on which the hydrodynamic journal bearing forces were evaluated by numerical solution of the Reynold's equation. In addition, the essential outputs of interest in this study, critical to determine wear rates are the tangential velocity and oil film thickness between the journals and bearing sleeve, which if not maintained appropriately, have a detrimental effect on the bearing performance.

Archard's wear prediction model was used in the simulation to calculate the wear rate of bearings with specific location information as all determinative parameters were obtained with reference to crank rotation. Oil film thickness obtained from the model was used as a criterion to determine if the lubrication is sufficient to prevent contact between the journal and bearing thus causing accelerated wear. A limiting value of 1 μm was used as the minimum oil film thickness needed to prevent contact. The increased wear rate with growing severity of operating conditions is analogous and comparable to the rise in amplitude of the squared envelope of the referenced vibration signals. Thus on one hand, the developed model demonstrated its capability to explain wear behaviour and on the other hand it also helps to establish a co-relation between wear based and vibration based analysis. Therefore, the model provides a cost effective and quick approach to predict the impending wear in IC engine bearings under various operating conditions.

***Keywords*—**Condition monitoring, IC engine, journal bearings, vibration analysis, wear prediction.

I. Introduction and Background

JOURNAL bearings used in the big end of the connecting rod in IC engines are often subjected to wear coming from the unsteady operating conditions of the engine, such as, frequent start/stops, involvement of high temperatures and pressures, load and speed fluctuations [1], [2]. Therefore, operation of reciprocating machinery is far more complex than for rotating machines, which are rather stable. Thus the journal bearings used in IC engines are more likely to fail sooner than the rated life [3], [4]. The force generated by the combustion and the impulsive inertia is transmitted straight through the connecting rod, which is supported by the journal bearings, making them vulnerable to wear off as the impulsive load increases. The main challenge in identifying any abnormality in bearing performance is to understand the wear mechanism and have a beforehand knowledge of any approaching failure to predict the remaining life of the bearing. Visual inspection of journal bearings needs complete dismantling of the engine and is not an ideal method to detect faults in the early stages [5] as damages may be caused in the process.

Vibration and wear debris analysis techniques are commonly used in industry for fault detection in machine elements. However limited success has been reported on the application of these techniques for fault detection in big end bearings, because of the complexity of resulting vibration signals and highly intrusive, labour, time and cost intensive experimental work involved [6].

Wear based analysis provides sufficient information on the wear mechanisms and insight on the effect of wear on bearing performance, whereas vibration analysis is good at detecting abnormalities in operation regardless of the cause of the fault. Thus, if the two techniques could be correlated together, then it would results in an effective condition monitoring by integrating the features of instantaneous vibration based diagnosis and wear debris analysis based root cause analysis and prognosis [7]. As discussed earlier the identification of mechanical faults in IC engines is a tedious task, therefore lot of recent researches has been directed towards developing simulation models to mimic fault indicators such as vibration signals and wear behaviour. A broad review on common engine faults, their indicators and challenges in identifying them experimentally is given in [8].

This work is an extension of a previous study, in which an engine simulation model was developed using a MATLAB/SIMULINK program, whereby the engine parameters used in the simulation were obtained experimentally from a Toyota 3SFE 2.0 litre petrol engine. Simulated hydrodynamic bearing forces were used to estimate vibrations signals and envelope analysis was carried out to analyze the effect of speed, load, and clearance on the vibration response. Three different loads 50/80/110 N-m, three different speeds 1500/2000/3000 rpm, and three different clearances, i.e., normal, 2 times and 4 times the normal

M. D. Haneef is with the Mechanical Engineering Department at the University of New South Wales, Kensington, NSW 2052, Sydney, Australia (phone: +61293854093; fax: +61296631222; e-mail: m.haneef@student.unsw.edu.au).

R. B. Randall and Z. Peng are with the Mechanical Engineering Department at the University of New South Wales, Kensington, NSW 2052, Sydney, Australia (phone: +61293854093; fax: +61296631222).

clearance were simulated to examine the effect of wear on bearing forces. The magnitude of the squared envelope of the generated vibration signals though not affected by load, but it was observed to rise significantly with increasing speed and clearance indicating the likelihood of augmented wear.

The simulation of engine mechanism with a clearance at joint (connecting rod big end bearing), is an interesting multi-body dynamics problem as the motion of the components involved is constrained by dynamic forces developed during operation and not the geometry. Since the elementary mechanism of engine is based on slider-crank mechanism, various studies have been reported in literature on developing the kinematics/kinetics of slider-crank mechanism with a revolute joint with clearance at either of the ends or both.

Flores presented a comprehensive study on the dynamics of slider-crank mechanism with lubricated revolute joint, whereby Reynold's equation was used to obtain the forces, and then compared with ideal joint [9]. In this work, however the combustion force effects were not taken into account. In that study several lubrication models and boundary conditions were studied, with different oil viscosities and clearances and the resulting bearing forces were compared with experimental results. A few other prominent studies on lubricated joints are also available [10]-[12]. However, the scope of most of the available researches is limited to investigating the effect of geometric parameters, such as size and clearance of bearings (though usually not with oversized clearance). Operating parameters such as oil viscosity and speed on the forces developed in clearance joints based on different lubrication and/or contact models but very few studies are available that encompass the use of the generated forces for wear prediction [13], [14]. Most of the wear prediction models are based on dry contact without taking into account the lubrication between the sliding parts. Nikolic [15] presented a simulation implementation algorithm to predict wear profiles for the crankshaft main bearings (which is rather even than the big end bearings) for a multi-cylinder engine operated at different conditions. Various aspects contributing towards the wear, including contact angle, contact pressure, effect of forces form neighbouring cylinders and location of wear zones with respect to crank rotation were studied in detail, however the clearance joint was assumed dry, without taking into account the lubrication effect. However, the implementation strategy provides with a promising prospect for wear predictions. Various other studies are available in literature, on the simulation of forces developed in joints with clearances (lubricated and/or dry) and predicting wear based on different indicators. A comprehensive review on similar multibody dynamics cases with joint clearances is presented in [16].

As mentioned earlier, this work is motivated by a recent study [17], which presented the simulation of vibration signals generated due to bearing knock, and evaluated by using envelope analysis. The simulated results were also compared with experimental results and were found to be in good agreement. Envelope analysis has proved to be successful in identifying underlying periodicity in impulsive vibration responses and thus can be an indicator of bearing knock occurring at regular intervals. It has proven to be an appropriate technique for fault detection in IC engine bearings. In envelope analysis the envelope of the signal is obtained by amplitude demodulation rather than using the raw signal and then the characteristic fault frequencies are identified [18]. The reason for the adoption of this method is its ability to deal with transient signals with slight phase differences which is often the case in machinery [19]. Various studies are available in the literature that demonstrate the successful use of envelope analysis for fault detection in machine elements particularly in rolling element bearings [20].

The present study expands the reference simulation model given in [17] with major emphasis on wear prediction and comparing the results with simulated and experimental vibration analysis results reported earlier. This work focuses and demonstrates the capability of the engine simulation model to obtain critical parameters mainly responsible for wear and further probe into the wear behaviour and the declining of bearing performance. In addition to material properties, the parameters of interest that contribute to wear are the load on the bearings *(F_{xy}),* the sliding velocity *(U),* oil film thickness *(h)* between the journal and the bearing sleeve, all of which are an output of the expanded simulation model. It is worth mentioning that all of the above parameters were obtained in reference to crank angle (θ) to reveal the location specific wear information for each case.

II. Engine Dynamics and Hydrodynamic Lubrication Model

Since the output of the engine, kinematics/kinetics (location of journal and bearing center and resulting eccentricity) is the input to the lubrication system, and the output of the lubrication system (bearing forces acting as constraint) is an input to the engine kinetic system. Hence forming a closed loop is thus crucial, the engine kinematics/kinetics is synchronized and works in conjunction with the hydrodynamic lubrication model that yields the constraining bearing forces.

The dynamics of the piston, connecting rod and crankshaft with rigid connection between piston and connecting rod, and clearance at the joint between the crankshaft and connecting rod, was adopted from typical models available in literature (fundamentally modelled as slider-crank mechanism) [21], [22]. An appropriate lubrication model for clearance joint (big end bearing), based on Reynold's equation for variable rotating loads was selected to simulate the bearing forces, oil film thickness and relative radial and tangential velocities of the journal and bearing for use in wear prediction model. The geometrical parameters, masses and moment of inertias of the components involved were obtained experimentally in previous study [17] from a Toyota 3SFE 2.0 litre petrol engine, and are listed in Table I.

The following sub-sections discuss only the key equations used in the simulation to determine the inputs and outputs of each subsystem and the interaction amongst them. For details of step-by-step analytical models for engine kinematics/ kinetics, interested readers may refer to [17], [22], [23].

TABLE I
ENGINE PARAMETERS FOR SIMULATION

Engine Parameters	Value	Unit
Bearing length (L_b)	0.02	m
Bearing radius (R_b)	0.024	m
Normal bearing clearance (c)	0.0001	m
Lubricating oil viscosity (μ)	0.03	Pa.s
Crank Radius (R)	0.043	m
MOI of crankshaft and flywheel (I_c)	0.1	Kg.m^2
Mass of connecting rod (m_b)	0.693	Kg
Center to center length of connecting rod (b)	0.135	m
Distance of connecting rod mass center (b_1)	0.09	m
MOI of connecting rod (I_b)	0.002	Kg.m^2
Mass of piston (m_p)	0.467	Kg

A. Cylinder Pressure

The cylinder pressure varies with operating conditions i.e. external load and speed, with foremost dependence on external load. Therefore, it has to be adjusted for each case to simulate engine behaviour running at different operating conditions. It is also worth pointing out that the combustion pressure has to be simulated carefully as it serves as a boundary condition for simulations running at different operating conditions. Using as reference, the available experimental data and engine power and torque curves, the cylinder pressures for different operating conditions were simulated by using the Wiebe's function. The cylinder pressure (P) as function of crank angle (θ) is given by [24]:

$$\frac{dP}{d\theta} = \frac{\gamma-1}{V}\frac{dQ}{d\theta} - \frac{P\gamma}{V}\frac{dV}{d\theta} \quad (1)$$

where, V is the volume of the cylinder, $dV/d\theta$ is the change in volume in terms of crank angle during piston displacements, and γ is the heat capacity ratio (~1.4 for air). The burn rate and the heat release rate in (1) during the combustion process were obtained in terms of the crank angular displacement (θ) by using:

$$w(\theta) = \frac{dx}{d\theta} = \frac{6.908(m+1)}{\theta_d}\left(\frac{\theta}{\theta_d}\right)^m e^{-6.908\,(\theta/\theta_d)^{m+1}} \quad (2)$$

$$\frac{dQ}{d\theta} = w(\theta)\, r_{com}\, m_{fuel}\, LHV \quad (3)$$

where, m is the Combustion characteristic exponent that determines the pressure curve shape, θ_d= combustion duration, LHV = Latent heat value (43900 KJ/Kg for petrol), r_{com} is the combustion efficiency of the engine and m_{fuel} is the mass of fuel injected in the cylinder for one combustion cycle. Thus, by substituting (2) and (3) in (1), the cylinder pressure variation with crank rotation was obtained. Fig. 1 shows the cylinder pressure for three different loads for one complete cycle (720 degrees of crank rotation) used in the simulation i.e. 50 N-m, 80 N-m and 110 N-m.

B. Piston-Connecting Rod Subsystem

The kinematic/kinetic relations for the piston connecting rod subsystem (modeled as an ideal joint) and crank subsystem with clearance between connecting rod and crankshaft joint, are established based on the configuration in Fig. 2.

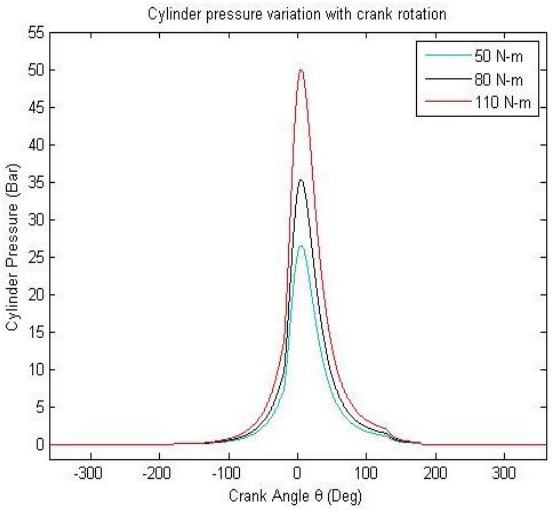

Fig. 1 Cylinder pressure vs crank rotation

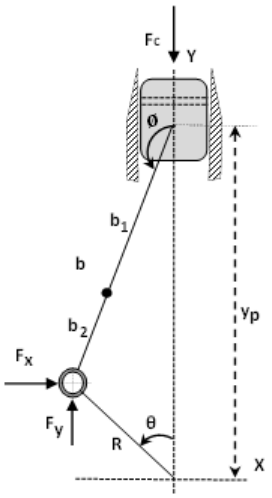

Fig. 2 Engine Kinematic/Kinetic diagram

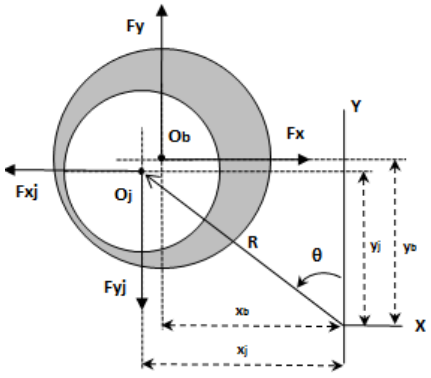

Fig. 3 Journal/bearing centers and force balance

The combustion force F_c serves an input to this subsystem

and as the driving force for the whole system and since the connection between the connecting rod and crank is not rigid but a revolute clearance joint, it has to be balanced by the hydrodynamic forces generated in the lubricating oil. The relative displacements of the journal and bearing centers i.e. x_b, y_b and x_j, y_j, respectively, with reference to global X-Y axes, and the balance of journal forces, F_{xj} and F_{yj} by the hydrodynamic forces generated by lubrication film F_x and F_y are shown in Fig. 3.

Based on the arrangement shown in Figs. 2 and 3, the governing equations of motion for piston and connecting rod can be obtained by Lagrange formulation as [23]:

$$(m_p + m_b)\,\ddot{y}_p - (b_1 m_b \sin\emptyset)\ddot{\emptyset} - \dot{\emptyset}^2 b_1 m_b \cos\emptyset = F_{y22} - F_c \quad (4)$$

$$(-b_1 m_b \sin\emptyset)\,\ddot{y}_p + (I_b + b_1^2 m_b)\ddot{\emptyset} = -F_{x22} b \cos\emptyset - F_{y22} b \sin\emptyset \quad (5)$$

C. Crank Subsystem

From the geometric relations shown in Fig. 3, the displacements, velocities, and accelerations of the x and y coordinates of bearing center are obtained, and finally the torque balance on the crankshaft can be written as:

$$I_c\ddot{\theta} = F_x R\cos\theta + F_y R\sin\theta + T_{fric} + T_{load} \quad (6)$$

where T_{load} is the external load on the engine and T_{fric} is the friction and pumping torque of the engine given by [25]:

$$T_{fric} = 0.697 + \dot{\theta} \times (2.995 \times 10^{-8}\, n - 1.487 \times 10^{-5}) V_d \quad (7)$$

D. Interaction Subsystem

To establish synchronization between the engine kinematics and the journal bearing dynamics it is important to develop relation between their geometric features. Fig. 4 shows the geometry of the big end bearing with a local coordinate system r-t in radial and tangential directions, and it is concurrence with the global X-Y coordinate system.

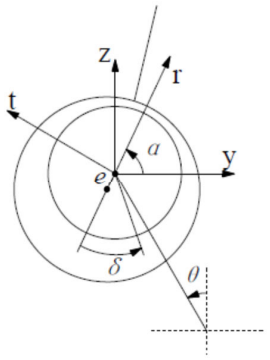

Fig. 4 Global and local coordinate system for big end bearing [17]

Based on the calculated displacements of journal and bearing centers from the piston-connecting rod and crank subsystems Fig. 3, the eccentricity the x and y direction is obtained as:

$$e_x = x_j - x_b \quad (8)$$

$$e_y = y_j - y_b \quad (9)$$

Therefore, the eccentricity is,

$$e = \sqrt{{e_x}^2 + {e_y}^2} \quad (10)$$

By using the bearing clearance (c), thus the eccentricity ratio ε and time derivative of eccentricity ratio ε̇ can be calculated as

$$\varepsilon = \frac{e}{c} \quad (11)$$

$$\dot{\varepsilon} = \frac{(y_b - y_j)(\dot{y}_b - \dot{y}_j) - (x_b - x_j)(\dot{x}_b - \dot{x}_j)}{e.c} \quad (12)$$

The transformation angle α from global X-Y to r-t coordinate system is calculated in terms of sine and cosine (to avoid complications that could arise from the tangent) and it's time derivative α̇ respectively as,

$$\sin(\alpha) = \frac{(y_b - y_j)}{e} \quad (13)$$

$$\cos(\alpha) = \frac{(x_b - x_j)}{e} \quad (14)$$

$$\dot{\alpha} = \frac{(x_b - x_j)(\dot{y}_b - \dot{y}_j) + (y_b - y_j)(\dot{x}_b - \dot{x}_j)}{e^2} \quad (15)$$

The above coordinate transformations will be used in hydrodynamic lubrication model discussed in the next section, after the following substitutions for simplification purpose:

$$E = \frac{2}{\bar{\omega}}\,\dot{\varepsilon} \quad (16)$$

$$G = \frac{2}{\bar{\omega}}\,\dot{\alpha} \quad (17)$$

$$k = (1 - \varepsilon^2)^{1/2}\left[\left(\frac{1-G}{E}\right)^2 + \frac{1}{\varepsilon^2}\right]^{1/2} \quad (18)$$

where $\bar{\omega}$ is the relative angular velocity of journal and bearing.

E. Hydrodynamic Lubrication Model

The governing equation to model the pressure profile is the classic Reynold's equation. Since the big end bearings in IC engines are subjected to loads that vary in both magnitude and direction, the most appropriate model for hydrodynamic forces for variable rotating loads was adapted from Pinkus [26]. By numerically integrating the hydrodynamic pressure profile over the positive region (Gümbel boundary conditions), the hydrodynamic bearing forces in r and t direction can be acquired as follows:

For E>0 (i.e. Journal approaching the bearing surface)

$$F_r = \frac{-6\pi\varepsilon(1-G)}{(2+\varepsilon^2)(1-\varepsilon^2)^{1/2}}\left(\frac{k+3}{k+3/2}\right)\sin\alpha - \frac{3E}{(2+\varepsilon^2)(1-\varepsilon^2)^{3/2}} \times \left[4k\varepsilon^2 + (2+\varepsilon^2)\pi\left(\frac{k+3}{k+3/2}\right)\right]\cos\alpha \quad (19)$$

$$F_t = \frac{-6\pi\varepsilon(1-G)}{(2+\varepsilon^2)(1-\varepsilon^2)^{1/2}}\left(\frac{k+3}{k+3/2}\right)(-cos\alpha) - \frac{3E}{(2+\varepsilon^2)(1-\varepsilon^2)^{3/2}} \times \left[4k\varepsilon^2 + (2+\varepsilon^2)\pi\left(\frac{k+3}{k+3/2}\right)\right] sin\alpha \quad (20)$$

For E<0 (i.e. Journal distancing from the bearing surface)

$$F_r = \frac{-6\pi\varepsilon(1-G)}{(2+\varepsilon^2)(1-\varepsilon^2)^{1/2}}\left(\frac{k+3}{k+3/2}\right) sin\alpha + \frac{3E}{(2+\varepsilon^2)(1-\varepsilon^2)^{3/2}} \times \left[4k\varepsilon^2 - (2+\varepsilon^2)\pi\left(\frac{k+3}{k+3/2}\right)\right] cos\alpha \quad (21)$$

$$F_t = \frac{-6\pi\varepsilon(1-G)}{(2+\varepsilon^2)(1-\varepsilon^2)^{1/2}}\left(\frac{k+3}{k+3/2}\right)(-cos\alpha) + \frac{3E}{(2+\varepsilon^2)(1-\varepsilon^2)^{3/2}} \times \left[4k\varepsilon^2 - (2+\varepsilon^2)\pi\left(\frac{k+3}{k+3/2}\right)\right] sin\alpha \quad (22)$$

These forces are then transformed onto the global X-Y axes by using the following transformations:

$$F_x = \frac{1}{2}\frac{\mu\bar{\omega}}{\left(c/R_j\right)^2} R_b L_b \times F_r \quad (23)$$

$$F_y = \frac{1}{2}\frac{\mu\bar{\omega}}{\left(c/R_j\right)^2} R_b L_b \times F_t \quad (24)$$

The relative radial and tangential velocities of the journal and the oil film thickness are obtained respectively by:

$$U = R_b\bar{\omega} + c\dot{\varepsilon}sin\delta - c\varepsilon\dot{\beta}cos\delta \quad (25)$$

$$V = c\dot{\varepsilon}cos\delta + c\varepsilon\dot{\beta}sin\delta \quad (26)$$

$$h = c(1-\varepsilon cos\delta) \quad (27)$$

III. Numerical Simulation

The model was developed in MATLAB/SIMULINK program, based on above analytical models, whereby the engine parameters used, are listed in Table I and the initial conditions for the simulation are listed in Table II.

Based on the initial conditions and analytical model for the dynamics of the engine and bearing presented earlier, the simulation was developed in a closed loop form. The schematic of simulation with inputs and outputs of each subsystem is illustrated in Fig. 5.

TABLE II
Initial Conditions for Simulation

Parameters	Value	Unit
Crank Angle (θ)	0	rad
Crank angular velocity ($\dot{\theta}$)	315/210/156	rad/s
Connection rod angle ($\emptyset$)	pi	rad
Connecting rod velocity ($\dot{\emptyset}$)	-100.3/-66.9/-49.7	rad/s
Piston position in Y (y_p)	0.178	m
Piston velocity in Y ($\dot{y}_p$)	0	m/s

The second order ODEs, for engine kinetics were solved by a variable time step solver ODE45 (dortmund – prince) in Simulink, with a minimum time step of $1x10^{-10}$ and a maximum time step of $2x10^{-7}$. The simulation was run for duration of 0.3 sec with a fixed sampling interval of $5x10^{-5}$ s (200 kHz sampling frequency).

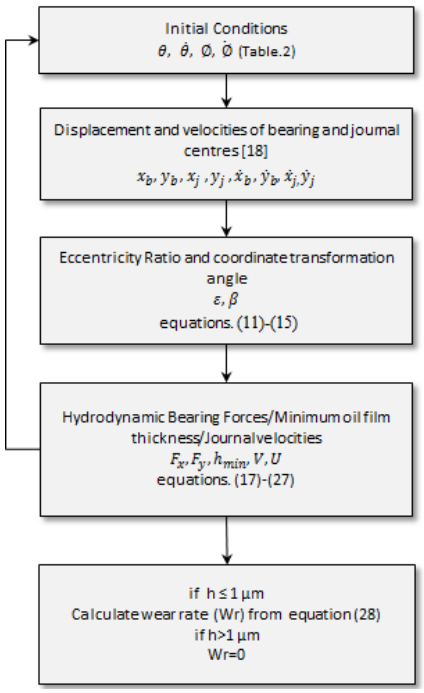

Fig. 5 Schematic of simulation implementation algorithm

IV. Results and Discussions

Unlike, the reference model [17], which mainly focused on vibration analysis by using simulated forces, the major outputs of interest in the present simulation is the resultant hydrodynamic bearing force (F). Sliding/tangential velocity (U), radial journal velocity (V), and the minimum oil film thickness (h_{min}) for a set of different operating conditions, with particular focus on investigating location specific wear rates. Since increased clearance is an indicator of wear, to simulate bearing forces for worn out bearing, two different clearance 2 times the normal (2x) and 4 times (4x) the normal clearance were used and compared with the results of bearing with normal clearance as a reference. The simulations were run at three different speeds i.e. 1500 rpm, 2000 rpm and 3000 rpm and three different loads of 50 N-m, 80 N-m and 110 N-m and compared. In all, with three combinations of each, the clearance, speed and load, 27 simulations were run and the results were compared. In following sub-sections, results and discussion of some important outcomes and their comparisons are presented. Details of all 27-simulation conditions and a summary of all results are presented in Table III.

The effect of each operating parameter speed, load and clearance on the bearing force, oil film thickness and tangential/sliding velocity of the journal is studied individually in following subsections (A-C), and then based on the results of oil film thickness, critical cases are analysed for determining wear rates in subsection-D.

A. Effect of Speed on Forces/Oil Film Thickness/Velocities

The resultant hydrodynamic bearing forces for two complete cycles of engine at three different speeds

(1500/2000/3000 rpm) with a load of 80 N-m, and 2 times the normal clearance are shown in Fig. 6. The corresponding position of the piston is marked as TDC (Top dead center) and BDC (Bottom dead center), as this information is crucial to suffice for identifying wear location on the bearing.

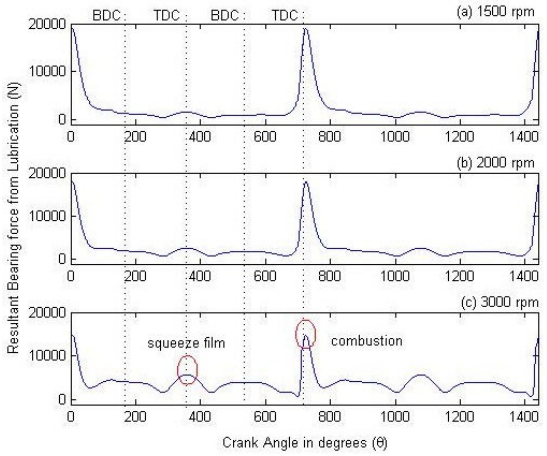

Fig. 6 Variation of resultant lubrication force with speed (80 N.m/c=0.0002) (a) 1500 rpm (b) 2000 rpm (c) 3000 rpm

The higher peaks occurring at every 720° of crank rotation (TDC) corresponds to the impulse due to combustion that follows every two complete revolutions of the crank. The magnitude of the higher peaks almost remain stable for different speeds but change with increase in external load, however the smaller humps due to squeeze film effect of lubricant (circled in red), corresponding to the bearing knock, grow in magnitude significantly with increasing speed, thus indicating added exposure to accelerated wear. A similar pattern was observed with all bearing clearances and loads with varying speed.

Oil film thickness was used as defining criteria to determine wear zones subjected to highest wear. Though being dependent on various factors, including size and geometry of bearings and lubricant properties, a limiting value of $h_{min} \leq 1$ um is selected as a criteria for considering boundary lubrication with high wear severity [27]. Around the clearance circle, to calculate wear, Archard's wear prediction model was applied in regions where the oil film thickness falls below 1 μm, indicating insufficient lubrication, consequently showing likelihood of observing higher wear rates. However, since an adequate lubricant film (h>1 μm) was observed in simulations with all cases of normal clearances, and no significant wear was observed at low of 1500 rpm even at 2 times the clearance. So major focus of the wear calculation is based on simulations running at 2000 rpm and 3000 rpm and/or with oversized increased clearance, where the fluid film breaks. Accordingly, the thickness of oil film has to be examined closely to determine if wear is induced in zones of minimum oil film thickness for instance of high speed and oversized clearance. For later use in the wear prediction model, the corresponding oil film thickness *h,* and the tangential and radial velocities of the journal U and V respectively for the case of 3000 rpm from Fig. 6 (c) are given in Fig. 7.

For the sake of comparison with results presented in Fig. 7, simulation results for same load and clearance i.e. 80 N.m/0.0002 m, but with a lower speed of 2000 are presented in Fig. 8.

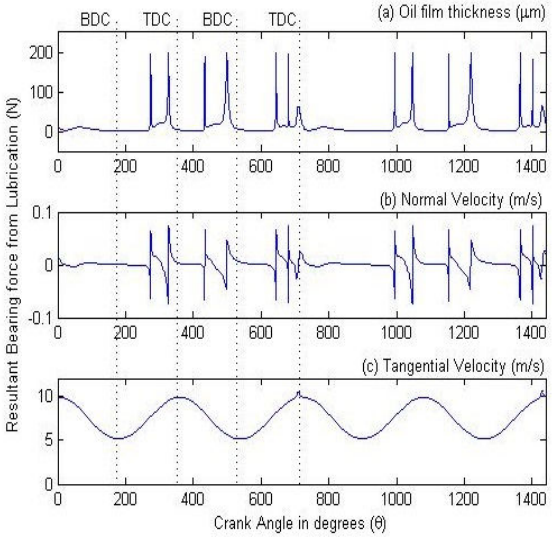

Fig. 7 Correspondence of oil film thickness/radial velocity/tangential velocity for 3000 rpm/80 N-m/c=0.0002 m (Fig. 6 (c)) (a) Oil film thickness μm (b) Normal Velocity m/s) (c) tangential Velocity (m/s)

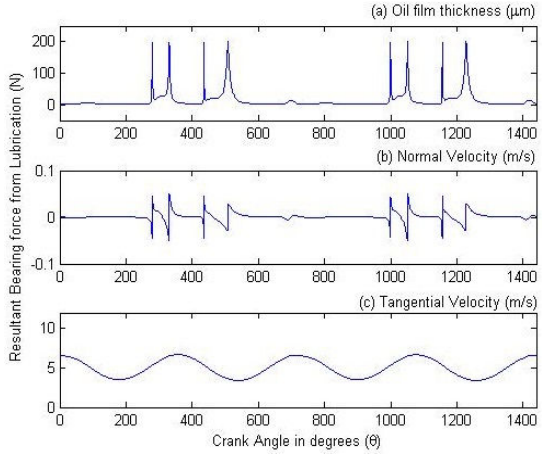

Fig. 8 Correspondence of oil film thickness/radial velocity/tangential velocity for 2000 rpm/80 N-m/c=0.0002 m (a) Oil film thickness μm (b) Normal Velocity m/s) (c) tangential Velocity (m/s)

Figs. 7 and 8 show a comparison of oil film thickness, normal velocity and tangential velocities for two cases with same load and clearance but different speed. In both of the cases, the oil film thickness dropped below 1 μm, therefore both were chosen for wear analysis. However, the magnitudes of the maximum normal and tangential velocities differ significantly for both cases.

$$U_{3000} = 10.5508 \text{ m/s}, U_{2000} = 6.7012 \text{ m/s}$$

$V_{3000} = 0.0743$ m/s, $V_{2000} = 0.0498$ m/s

Therefore based on the magnitudes of forces for both cases of Figs. 7 and 8 at points of minimum oil film thickness, and the normal and tangential velocities, it can be easily concluded that the wear rate observed by (28) in next section, will be much higher for the case of higher speed. Furthermore, it is also observed that the sudden change in oil film thickness happens where the forces change direction or sudden impulses occur, when the piston passes the TDC or BDC (every 180° of crank rotation). Similarly, an abrupt change in normal velocity of the journal is observed at same locations where the film thickness changes instantly. The tangential velocity, however, varies smoothly in a periodic manner with minor fluctuations at completion of each cycle. Similar coherence among the forces, oil film thickness, radial and tangential velocities is observed for all other operating conditions. It is worth mentioning that the parameters discussed above are crucial for determining the wear generated in the bearing with explicit location information as all the parameters are phase locked to the crank angle.

The existence of minimum oil film thickness at the instant the piston passes through the TDC or BDC (except in firing stroke where oil film is not minimum due to counteracting inertial effects), is an upfront indication. According to the bearing phase information with reference to the crank angle, the top and bottom surface of the bearing along the piston displacement axis are exposed to major wear.

B. Effect of Load on Forces/Oil Film Thickness/Velocities

Fig. 9 illustrates a comparison of forces when the bearing is subjected to operation at the same speed (i.e. 3000rpm) and clearance (0.0002m), but with changing external load/torque.

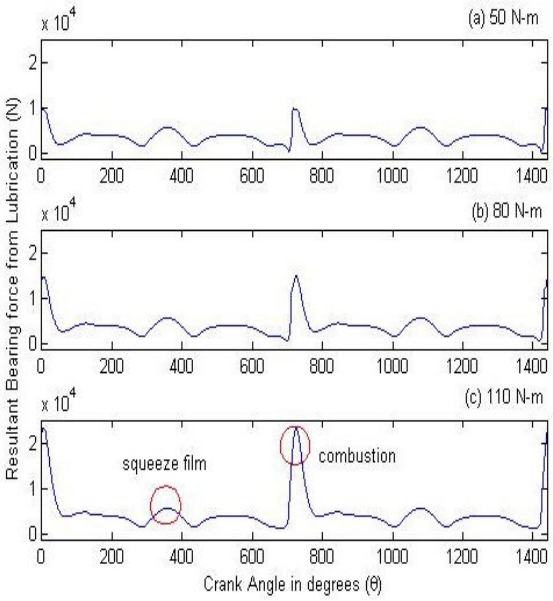

Fig. 9 Variation of resultant lubrication force with load (constant speed 3000 rpm/c=0.0002)

The combustion peaks stirring in this case changes in magnitude with increasing load; however, interestingly the small humps due to the squeeze film action of lubricant film do not rise considerably with load. This is owing to the fact that bearing knock forces are mainly attributed to the inertial effects rather than combustion effects. Thus, it is concluded that the bearing forces are not dominant by the external load on the engine, and the results confirmed by the vibration analysis results compared later in Section V. It is not necessary to illustrate the corresponding variation of oil film thickness, radial and tangential velocities of journal as a similar correlation is observed as were in case for variable speed analysis in the previous section.

C. Effect of Increased Clearance on Forces/Oil Film Thickness/Velocities

An oversized bearing clearance is an indicator of bearing wear. Thus to simulate the bearing with worn geometry different clearances were used in the simulation and the variation in results was studied. Fig. 10 shows the variation of forces with increasing clearance under harsh operating condition of 3000 rpm and 110 N-m:

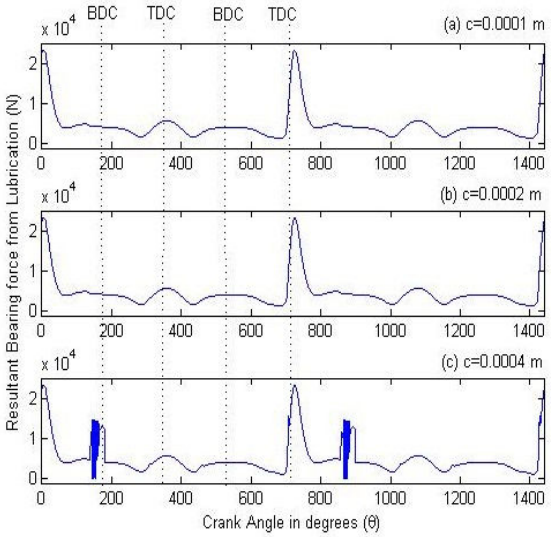

Fig. 10 Variation of resultant lubrication force with clearance (constant speed 3000 rpm/load 110 N-m) (a) normal clearance (b) 2x clearance (c) 4x clearance

For the case of 4x clearance the oil film starts to break near 180˚ when the piston passes the bottom dead center, as the oil film thickness in this region (marked in red rectangular area) is as low as h_{min}= *0.32459 μm*, and thus no longer able to support the load on the bearing. This region is thus susceptible to highest amount of wear, fast tracking the deterioration of the bearing. Similar to previous sections a plot of associated journal velocities and oil film thickness was generated corresponding to each operating condition, for later use in wear prediction model.

Depending on the results of above comparisons, it was observed that speed and oversized clearance plays an

important role in influence bearing knock, due to a considerable drop in oil film thickness, hence causing wear. Load however did not display any notable effect on reduction on oil film thickness for any of the combinations.

For further analysis to predict wear rates, the critical cases with high speed (2000/3000 rpm) conjoining with oversized clearances were selected, as the film thickness is found to be below the selected limit of 1μm.

D. Wear Rate Determination

Based on the parameters collected as above from the simulation model, the wear rate of the journal bearings can be predicted by using Archard's wear model [28]

$$W_r = k \frac{F \cdot U}{H} \quad (28)$$

where, W_r is the instantaneous wear rate *(mm³/s)*, *F* simulated is the bearing force (*N*), *U* is the tangential/sliding velocity (*m/s*), *H* is the hardness of the softer material (bearing sleeve in this case) and is selected as 186 HV, and *k* is the wear coefficient. The wear coefficient is dependent on several factors and not easy to determine. However, since the aim of this study is to highlight the location specific wear and its instigating dynamic information, so a same value of *k* (=7x10^{-3} mm^3/Nm) is used for all conditions [29].

Fig. 11 shows a comparison between the variation of oil film thickness and the corresponding wear with location information corresponding to crank angle and piston position, for the most overstated case of 3000 rpm/110 N-m/4x clearance.

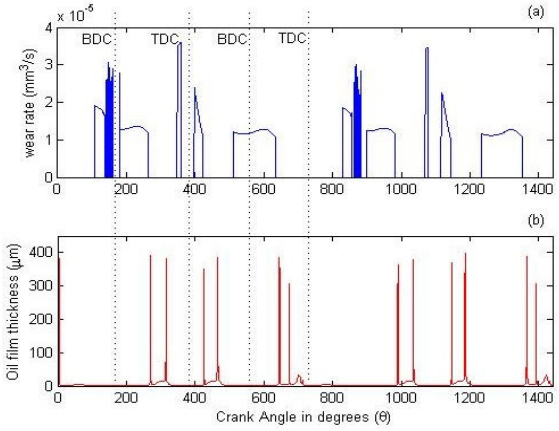

Fig. 11 Variation of wear rate with oil film thickness (speed 3000 rpm/load 110 N-m/clearance 0.0004 m) (a) Wear rate vs crank angle (b) Oil film thickness vs crank angle

It is evident that the wear rate is almost negligible where the oil film thickness is maximum (red peaks) whereas the wear rate hikes in zones where the oil film thickness is minimum, thus no longer being able to maintain sufficient lubrication. Same consistency between the trends of oil film thickness and wear rate was observed for all operating conditions.

It is discussed previously that wear is highly likely to occur on top or bottom edge of the bearing when the piston passes through TDC or BDC. However, for the sake of comparison and based on the assumption that the bearing forces and sliding velocity are time dependent, and during starts/stops and prolonged operation the bearing may wear uniformly. The instantaneous wear rate shown above was averaged over the cycles to get the averaged wear rate for one complete cycle [30], and the values listed in Table III.

Summarizing from Table III, in first 9 simulations at 1500 rpm no wear was observed at normal and 2 times the clearance, but a small amount of wear is observed only with 4 times the clearance, as the oil film thickness was found to be less than 1 μm. For the simulations running at 2000 rpm and 3000 rpm oil film thickness was found to be maintained sufficiently for normal clearance thus giving no indication of wear, but for 2x and 4x clearances at 2000/3000 rpm some wear is indicated with higher severity at 3000 rpm. The plot of wear rates from above table is presented in Fig. 12.

TABLE III
ALL SIMULATIONS AND OUTCOMES

No.	Speed	Load	c	Wear Rate (mm³/s)
1	**1500 rpm**	50 N-m	Nor	*0*
2			2x	*0*
3			4x	*7.55E-07*
4		80 N-m	Nor	*0*
5			2x	*0*
6			4x	*7.91E-07*
7		110 N-m	Nor	*0*
8			2x	*0*
9			4x	*1.06E-06*
10	**2000 rpm**	50 N-m	Nor	*0*
11			2x	*3.00E-07*
12			4x	*1.26E-06*
13		80 N-m	Nor	*0*
14			2x	*2.40E-07*
15			4x	*1.32E-06*
16		110 N-m	Nor	*0*
17			2x	*2.06E-07*
18			4x	*1.98E-06*
19	**3000 rpm**	50 N-m	Nor	*0*
20			2x	*1.40E-06*
21			4x	*3.31E-06*
22		80 N-m	Nor	*0*
23			2x	*1.39E-06*
24			4x	*3.29E-06*
25		110 N-m	Nor	*0*
26			2x	*1.65E-06*
27			4x	*3.39E-06*

The overall trend of wear rate (from condition 1-27) is escalating as the operating conditions (mainly speed and clearance) become tougher, implying a higher wear rate at higher speed and oversized clearance conditions. The first three points along the inclination of each individual peak represents the upsurge in wear rate with increasing clearance, thus indicating that once the wear is initiated in a normal bearing, the process is vigorously advanced.

V. Comparison with Vibration Analysis

A comprehensive study, on experimental and simulated vibration signals for same engine parameters and operating conditions, from a similar simulation model is presented by [17]. Based on the simulated bearing forces, vibration signals were extracted in the time domain by using experimentally determined frequency response functions (FRF). The vibration signals were used to identify bearing knock when the engine is running under different operating conditions. An example of simulated time domain signals at 3000 rpm/80 N-m/4x clearance (condition 24) is shown in Fig. 13.

Squared envelope analysis was performed on all acquired vibration signals and an increase in amplitude was reported with increasing speed and clearance, thus indicating the likelihood of advanced wear at exaggerated operating conditions.

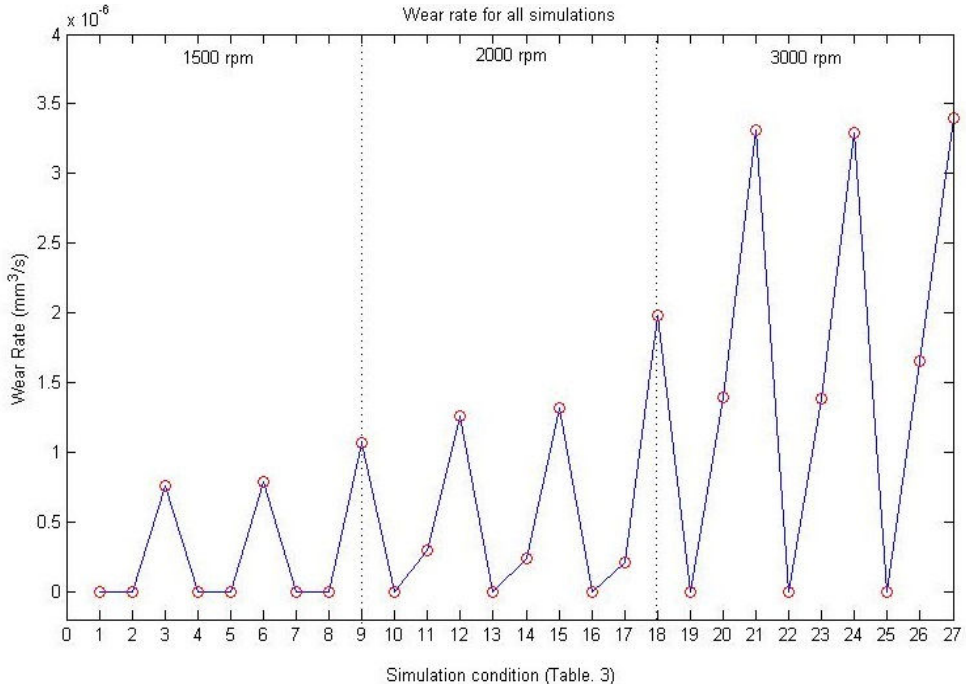

Fig. 12 Wear rate (W_r) for all 27 operating conditions

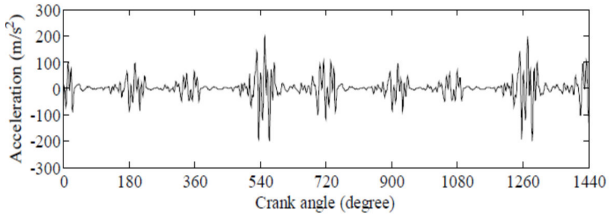

Fig. 13 Simulated vibration signal (condition 24) [17]

The corresponding squared envelope for the case shown above is given in Fig. 14.

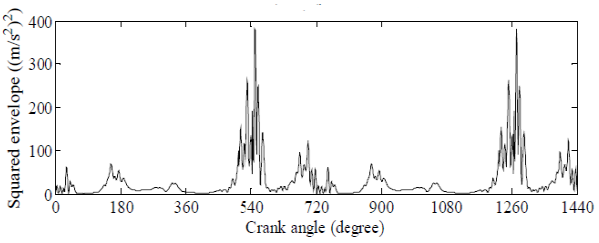

Fig. 14 Squared envelope signal (condition 24) [17]

In Fig. 14, the higher peaks occurring at regular intervals of 720° (corresponding to cylinder 2 as per the firing order 1-3-4-2) are the indicator of bearing knock, with increasing amplitude conforming to increase of speed and clearance, which is in comprehensive consistency with the wear rates predicted in current study. It should be noted that vibration amplitude is a much more sensitive measure of bearing force than calculated oil film thickness, which is insensitive when very small.

It is worth mentioning that the envelope analysis did not reported detection of bearing knock at lower speeds, and the major comparison was based on cases with higher speed and oversized clearances. Similar trend is confirmed by wear analysis in present study as it did not displayed any prominent wear due to the adequacy of oil film for low speed conditions.

VI. Conclusion

The presented work demonstrates the capability of a simulation model to investigate the crucial parameters that are detrimental for bearing performance, based on which the wear rates for different operating conditions were obtained. Experimental investigation of IC engine bearings is time

consuming and cost intensive, therefore appropriate simulation models can provide a better alternative to understand bearing wear phenomena by using oil samples and vibration signals as indicators. The wear rates obtained show the potential for developing a wear model based on combining vibration responses with wear debris analysis. Good agreement between simulated and measured response vibrations in a previous study indicated that simulated as well as measured vibration signals can be good indicators of wear progression and could lead to a more integrated methodology by combining wear and vibration measurement and simulation to give improved wear prediction models and thus improved prognostic ability. However, to establish correlation between vibration and wear based analysis, further experiments and simulations at higher speeds to generate more data, are necessary, as the recommended methods lack in providing relevant information at lower speeds. The simulation model can be improved further by including the mixed lubrication, and boundary lubrication regime, in addition to the Reynold's equation governing the full film lubrication in this model.

REFERENCES

[1] Jones MH. Wear Debris Associated with Diesel Engine Operation. Wear 1983; 90: 75-88.
[2] Geng Z, Chen J. Investigation into Piston-Slap-Induced Vibration for Engine Condition Simulation and Monitoring. Journal of Sound and Vibration 2005; 282: 735-51.
[3] Taylor C. M. Automobile Engine Tribology—Design Considerations for Efficiency and Durability. Wear 1998; 221: 1-8.
[4] Dufrane K. F., Kannel J. W., McCloskey TH. Wear of Steam Turbine Journal Bearings at Low Operating Speeds. Journal of Lubrication Technology 1983; 105.
[5] Cumming ACD. Condition Monitoring Today and Tomorrow—An Airline Perspective. In: Rao RKN, Au J, Griffiths B, editors. Condition Monitoring and Diagnostic Engineering Management: Springer Netherlands; 1990. p. 1-7.
[6] Antoni J., Daniere J, Guillet F. Effective Vibration Analysis OF IC Engines Using Cyclostationarity. Part I-A Methodology for Condition Monitoring. Journal of Sound and Vibration 2002; 257: 815-37.
[7] Peng Z., Kessissoglou NJ, Cox M. A Study of the Effect of Contaminant Particles in Lubricants Using Wear Debris and Vibration Condition Monitoring Techniques. Wear 2005; 258: 1651-62.
[8] Jones N. B, Li Y-H. A Review of Condition Monitoring and Fault Diagnosis for Diesel Engines. Tribotest 2000; 6: 267-91.
[9] Flores P, Ambrósio J, Claro JCP, Lankarani HM, Koshy CS. Lubricated Revolute Joints in Rigid Multibody Systems. Nonlinear Dyn 2009; 56: 277-95.
[10] Flores P., Ambrósio J., Claro J. C. P., Lankarani HM. Kinematics and Dynamics of Multibody Systems with Imperfect Joints: Models and Case Studies: Springer Berlin Heidelberg; 2008.
[11] Schwab A. L., Meijaard J. P., Meijers P. A Comparison of Revolute Joint Clearance Models in the Dynamic Analysis of Rigid and Elastic Mechanical Systems. Mechanism and Machine Theory 2002;37:895-913.
[12] Erkaya S, Uzmay İ. Experimental Investigation of Joint Clearance Effects on the Dynamics of a Slider-Crank Mechanism. Multibody Syst Dyn 2010; 24: 81-102.
[13] Mukras S, Mauntler N, Kim NH, Schmitz T, Sawyer WG. Dynamic Modeling of a Slider-Crank Mechanism under Joint Wear. ASME 2008 International Design Engineering Technical Conferences and Computers and Information in Engineering Conference: American Society of Mechanical Engineers; 2008. p. 443-52.
[14] Bai ZF, Zhang HB, Sun Y. Wear Prediction for Dry Revolute Joint with Clearance in Multibody System by Integrating Dynamics Model and Wear Model. Latin American Journal of Solids and Structures 2014; 11: 2624-47.
[15] Nikolic N, Torovic T, Antonic Z. A Procedure for Constructing a Theoretical Wear Diagram of IC Engine Crankshaft Main Bearings. Mechanism and Machine Theory 2012; 58: 120-36.
[16] Gummer A, Sauer B. Modeling Planar Slider-Crank Mechanisms with Clearance Joints in RecurDyn. Multibody Syst Dyn 2014; 31: 127-45.
[17] Chen J, Randall R, Feng N, Peeters B, Van der Auweraer H. Modelling and Diagnosis of Big-End Bearing Knock Fault in Internal Combustion Engines. Proceedings of the Institution of Mechanical Engineers, Part C: Journal of Mechanical Engineering Science 2014; 228: 2973-84.
[18] McFadden P. D, Smith J. D. Vibration Monitoring of Rolling Element Bearings by the High-Frequency Resonance Technique—A Review. Tribology International 1984; 17: 3-10.
[19] Randall RB, Antoni J, Chobsaard S. The Relationship between Spectral Correlation and Envelope Analysis in the Diagnostics of Bearing Faults and Other Cyclostationary Machine Signals. Mechanical Systems and Signal Processing 2001; 15: 945-62.
[20] Rubini R, Meneghetti U. Application of the Envelope and Wavelet Transform Analyses for the Diagnosis of Incipient Faults in Ball Bearings. Mechanical Systems and Signal Processing 2001; 15: 287-302.
[21] Chi JN. Non-Invasive Diagnostics of Excessive Bearing Clearance in Reciprocating Machinery: Massachusetts Institute of Technology, Department of Mechanical Engineering; 1995.
[22] Chen J. Internal Combustion Diagnostics Using Vibration Simulation University of New South Wales, Australia 2013.
[23] Daniel GB, Cavalca KL. Analysis of the Dynamics of a Slider–Crank Mechanism with Hydrodynamic Lubrication in the Connecting Rod–Slider Joint Clearance. Mechanism and Machine Theory 2011; 46: 1434-52.
[24] Kakaee AH, Shojaeefard MH, Zareei J. Sensitivity and Effect of Ignition Timing on the Performance of a Spark Ignition Engine: An Experimental and Modeling Study. Journal of Combustion 2011; 2011: 8.
[25] Zweiri YH, Whidborne JF, Seneviratne LD. Detailed Analytical Model of a Single-Cylinder Diesel Engine in the Crank Angle Domain. Proceedings of the Institution of Mechanical Engineers, Part D: Journal of Automobile Engineering 2001; 215: 1197-216.
[26] Pinkus O, Sternlicht B. Theory of hydrodynamic lubrication. New York: McGraw-Hill; 1961.
[27] Mang T, Dresel W. Lubricants and Lubrication: Wiley; 2007.
[28] Archard JF. Contact and Rubbing of Flat Surfaces. Journal of Applied Physics 1953; 24: 981-8.
[29] Winer WO, Peterson MB. Wear Control Handbook: American Society of Mechanical Engineers; 1980.
[30] Mustafa Duyar ZD. Design Improvement Based on Wear of a Journal Bearing Using an Elastohydrodynamic Lubrication Model. International Compressor Engineering Conference, 2006.